# Coaxial Electrospun Fibermat of Poly(AM/DAAM)/ADH and PCL: Versatile Platform for Functioning Active Enzymes

Yuji Tanikawa, Yuya Ido, Ren Ando, Akiko Obata, Kenji Nagata, Toshihiro Kasuga, and Toshihisa Mizuno*

The core-shell fibermats, consisting of the core unit (prepared from the copolymer of acrylamide (AM) and diacetone acrylamide (DAAM), poly(AM/DAAM), and the bifunctional crosslinker, adipic acid dihydrazide (ADH)) and thin shell unit of poly(ε-caprolactone) (PCL) (or other hydrophobic polymer) could be used as effective enzyme-immobilizing platforms.

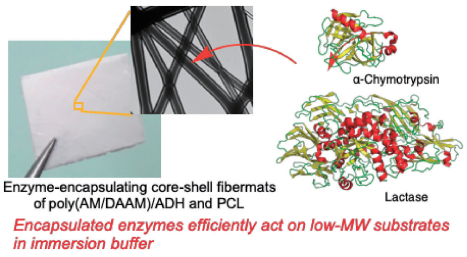


REPRINTED FROM

BCSJ Bulletin of the Chemical Society of Japan

Vol.93 No.10 2020 p.1155–1163

October 15, 2020

The Chemical Society of Japan

BCSJ

Document type: Article

# Coaxial Electrospun Fibermat of Poly(AM/DAAM)/ADH and PCL: Versatile Platform for Functioning Active Enzymes

**Yuji Tanikawa,[1] Yuya Ido,[1] Ren Ando,[1] Akiko Obata,[1] Kenji Nagata,[1] Toshihiro Kasuga,[1] and Toshihisa Mizuno*[1,2]**

[1]Department of Life Science and Applied Chemistry, Graduate School of Engineering, Nagoya Institute of Technology, Gokiso-cho, Showa-ku, Nagoya, Aichi 466-8555, Japan

[2]Department of Nanopharmaceutical Sciences, Graduate School of Engineering, Nagoya Institute of Technology, Gokiso-cho, Showa-ku, Nagoya, Aichi 466-8555, Japan

E-mail: toshitcm@nitech.ac.jp

Received: April 24, 2020; Accepted: June 4, 2020; Web Released: June 11, 2020

**Toshihisa Mizuno**
Toshihisa Mizuno received his Ph.D. from Kyushu University in 2000. He is currently an Associate Professor in the Department of Life and Applied Chemistry, Graduate School of Engineering, Nagoya Institute of Technology. His research interests include design of biomacromolecules and materials having biological functions.

## Abstract

In this study, we prepared and characterized enzyme (α-chymotrypsin or lactase)-encapsulating core-shell fibermats by electrospinning. The hydrophilic copolymer of acrylamide (AM) and diacetone acrylamide (DAAM), poly(AM/DAAM), was used as the base material to obtain the core unit of nanofibers. During electrospinning, poly(AM/DAAM) was crosslinked with the bifunctional crosslinker adipic acid dihydrazide (ADH) in the presence of enzyme molecules. The cores were wrapped with hydrophobic poly(ε-caprolactone) (PCL) layers as shell unit. Different from the fibermats of only poly(AM/DAAM)/ADH, the core-shell fibermat of poly(AM/DAAM)/ADH and PCL exhibited sufficient mechanical strength and stability of the stacked nanofibrous structure in a neutral-pH buffer. Furthermore, when the PCL-shell thickness was controlled to be less than 150 nm, the encapsulated enzymes exhibited an apparent activity of >70–80% for low-molecular weight substrates in an immersion buffer. These results indicate that the core-shell fibermats of poly(AM/DAAM)/ADH and PCL (or other hydrophobic polymer) could be used as effective enzyme-immobilizing platforms.

**Keywords:** Fibermat | Co-axial electrospinning | Protein-encapsulation

## 1. Introduction

The fabrication of electrospun fibermats, composed of nanofibers that can encapsulate functional biomacromolecules such as peptides, proteins, or nucleic acids, without any loss of the original biological functions, has attracted considerable research attention.[1] This is because biomacromolecule-encapsulating fibermats are considered favorable materials for designing cell-incubation scaffolds that allow control of cell proliferation and differentiation,[2,3] protein-drug delivery systems with controlled-release properties,[4–7] and enzyme-immobilizing supports.[4] Aiming at application to enzyme-immobilizing supports, the enzyme-encapsulating fibermats need to retain the nanofibrous scaffold structure even after being immersed in aqueous buffer for a certain period, since it is indispensable to exhibit efficient enzymatic functions even in nanofibers. To increase stability (water-insolubility and enough mechanical strength) of nanofibrous scaffold structure in aqueous solvents, choice of hydrophobic polymers for the base materials of fibermats seems a reasonable strategy. However, mixing enzyme molecules in organic solvents for preparing the precursor solution for electrospinning and/or further direct contact of enzyme molecules with hydrophobic polymers in the obtained fibermat nanofibers would cause serious damage in enzymatic functions. Therefore, several sophisticated preparation methods, compatible with maintenance of nanofibrous scaffold structure in aqueous solvents and decrease in damages to enzymatic functions, have been studied so far.

One of the methods able to provide the water-insoluble fibermats, encapsulating proteins with less damage, is emulsion electrospinning.[5] In this method, hydrophobic polymers such as poly(lactic acid) (PLA) are used as the base materials and an emulsion solution, formed by the hydrophobic polymer in



 

organic solvent and protein in aqueous buffer, is used for electrospinning. To reduce the protein structural damage and activity loss, Ca alginate,[5] methyl cellulose,[8] or gelatin[2] is a supplement added to the aqueous phases of precursor emulsion solution. The second one is the post-crosslinking method, in which post crosslinking treatments are applied to the beforehand-prepared water-soluble protein-encapsulated fibermats.[9] Several post-treatments have been studied to obtain water-insoluble fibermats including chemical crosslinking using bifunctional crosslinkers such as glutaraldehyde,[10] photoirradiation[11] or thermal treatments[12] in the presence of corresponding crosslinkers. However, to reduce damage to the encapsulated proteins, careful choice of reaction conditions is necessary.

As another new method to prepare enzyme-encapsulating fibermats, we recently reported the *in-situ* crosslinking during electrospinning (SCES) method. In this method, post-crosslinkable polymers and the corresponding bifunctional crosslinker ae used.[13–15] Because the spinning step of nanofibers via electrospinning includes a solvent volatilization process, we expected effective *in situ* crosslinking between post-crosslinkable polymers and the corresponding bifunctional crosslinker via dehydration condensation reaction during electrospinning. As result, by using the precursor aqueous solution of poly(γ-glutamate) (γ-PGA) and 3-glycidyloxypropyltrimethoxysilane (GPTMS), or the copolymer of acrylamide (AM) and diacetone acrylamide (DAAM) poly(AM/DAAM) and adipic acid dihydrazide (ADH), we successfully obtained water-insoluble protein-encapsulated fibermats from the precursor aqueous solution of water-soluble polymers and proteins. Since we could prepare the protein-encapsulating fibermats using only aqueous solvents, we successfully encapsulated the green fluorescent protein (GFP) and α-chymotrypsin (α-Chy) without denaturation.[15] Furthermore, because of the subtle porous structure of the polymeric network formed by γ-PGA/GPTMS and poly(AM/DAAM)/ADH, high-molecular weight (MW) enzyme proteins could be held in nanofibers without leakage but low-MW substrate molecules could permeate the nanofibers. As a result, the enzymatic activities of the encapsulated α-Chy were >85% of that of α-Chy (same amount) dissolved in a buffer. These findings showed that the protein-encapsulating fibermats fabricated using the SCES method could be potentially used for new types of methods to prepare enzyme-encapsulating fibermats. However, especially in case of poly(AM/DAAM)/ADH fibermats, the fibermats showed low mechanical strength and were fragile, insufficient for practical use as enzyme-immobilizing substrates. Further, because the covalent bonding between the ketone groups in poly(AM/DAAM) and the hydrazide groups in ADH is reversible, gradual fusion of adjacent nanofibers in the obtained fibermats was observed after long-term immersion in the buffer, which caused a reduction in the total surface area of the nanofibers against immersing solvents. Consequently, the activity of the encapsulated enzyme decreased over time.

In this study, to overcome the two aforementioned drawbacks of poly(AM/DAAM)/ADH fibermat, we modified it to the core-shell type fibermats,[16] wherein the protein-encapsulating poly(AM/DAAM)/ADH nanofibers were wrapped with thin hydrophobic layers of poly(ε-caprolactone) (PCL). Enhancement in stability of hydrophilic nanofibers by wrapping with a hydrophobic polymer, yielding core-shell fibermats was reported, so it should be a rational solution.[17] Application of core-shell fibermats to a protein (such as BSA, growth factor proteins, etc.)-loadable/releasable substrate was also reported.[18] However, enzyme encapsulation and detail evaluation of their biological activities was less reported. In this study, we therefore prepared the enzyme-encapsulating core-shell fibermats using a co-axial electrospinning technique and examined not only whether the wrapping of poly(AM/DAAM)/ADH nanofibers with PCL could effectively overcome the aforementioned drawbacks but also the relationship between the shell thickness and the apparent enzymatic reactivity of the encapsulating enzyme molecules.

## 2. Experimental

**Materials.** Unless stated otherwise, all chemicals and reagents were commercially obtained and used without further purification. Tris(hydroxymethyl)aminomethane (Tris), *p*-nitrophenyl acetate (*p*-NAc), *p*-nitrophenyl-β-D-glucopyranoside (*p*-NGlu), acrylamide (AM), 2,2,2-trifluoroethanol (TFE), 2,2′-azobis[*N*-(2-carboxyethyl)-2-methylpropionamidine] tetrahydrate (VA-057), disodium phosphate ($Na_2HPO_4$), sodium dihydrogen phosphate ($NaH_2PO_4$), fluorescein, and rhodamine B were purchased from Wako Pure Chemical Ind. Ltd. (Japan). 100 mM phosphate buffer (pH 8) was prepared by mixing 100 mM $Na_2HPO_4$ and 100 mM $NaH_2PO_4$. Diacetone acrylamide (DAAM) and adipic acid dihydrazide (ADH) were purchased from Tokyo Chemical Industry Co., Ltd. (Japan). DAAM was recrystallized several times from ethyl acetate to remove the inhibitor mequinol before use in reversible addition–fragmentation chain transfer (RAFT) polymerization.[19] α-Chy, Lac, PCL (number-average MW ($M_n$) = 80,000), and trypsin-chymotrypsin inhibitor (TCI) from *Glycine max* (soybean)[20] were purchased from Sigma-Aldrich (USA). Poly(AM/DAAM) featuring AM and DAAM at a molar ratio of 8:2 was synthesized as described; in our previous paper, poly(AM/DAAM) is described in the place of PAM-*co*-PDAAM.[15] The $M_n$ and polydispersity index (PDI) of poly(AM/DAAM) were determined using gel-permeation chromatography (GPC).

**Construction of Core-Shell Fibermats with/without Encapsulated Proteins or Fluorescent Molecules.** ADH (0.5 molar equiv. with respect to the DAAM unit in poly(AM/DAAM)) was added to a solution of poly(AM/DAAM) (0.5 g in 2.5 mL of 100 mM phosphate buffer, pH 8) and transferred into a Luer lock syringe (5 mL). When encapsulating proteins, such as GFP, α-Chy, or Lac, 5 wt% of the protein of interest (with respect to the mass of the polymer) was added to the solution. In the case of fluorescent molecules such as fluorescein and rhodamine B, 0.4 mmol was added to the solution. Concomitantly, 8 wt% PCL solution in TFE was prepared and transferred into another Luer lock syringe (5 mL). The two syringes were then placed in different syringe pumps fitted with a linear actuator (KDS-100, KD Scientific, USA) and connected to a coaxial spinneret (MECC Co. Ltd, Japan) with 27 G needle (Terumo Corp., for the core solution of poly(AM/DAAM)/ADH) through a PTFE tube. The aforementioned solutions were electrospun (SD-02, MECC Co. Ltd, Japan) at a linear extrusion velocity of 0.1 mL/h for the poly(AM/DAAM)/ADH solution and 0.4 mL/h for the PCL solution

under high voltage (25 kV). The core component of the obtained fibermat was poly(AM/DAAM)ADH and the shell component was PCL. The distance between the tip of the spinneret and the grounded collector (aluminum plate, 150 × 200 mm) was set to 150 mm.

**Scanning Electron Microscopy (SEM).** Samples were coated with amorphous osmium through plasma chemical vapor deposition by using a JEE-420T vacuum evaporator (JEOL, Japan). Sample morphologies were examined using field-emission SEM (JSM-6301F, JEOL, Japan). The mean diameters of the fibermat nanofibers and their standard deviations were evaluated from the SEM images of 30 nanofibers, using the software, Image J.

**Transmission Electron Microscopy (TEM).** Samples for TEM observation were prepared by directly collecting the spun core-shell nanofibers from the coaxial spinneret onto a TEM grid (Formvar Carbon Film on Copper 100 mesh (50), Okenshoji Co., Ltd, Japan). To obtain adequate image contrast between core and shell portions, sodium phosphotungstate was mixed into the core precursor solution of poly(AM/DAAM) and ADH at a final concentration of 0.001% (w/v). TEM images were acquired using a JEM-z2500 instrument (JEOL, Japan), under an acceleration voltage of 200 kV.

**Attenuated Total-Reflectance Fourier-Transform Infrared (ATR-FTIR) Spectroscopy.** ATR-FTIR spectra were acquired using an FT-IR-4000 spectrometer (JASCO, Japan) equipped with an ATR PRO450-S unit (JASCO, Japan). The FID spectra scanned 200 times at ambient temperature were accumulated and Fourier-transformed to obtain FTIR spectra at 4 $cm^{-1}$ resolution.

**Release Behavior of Encapsulated GFP from Core-Shell Fibermats under Different pH Conditions.** Stability of core-shell fibermats upon immersion in buffers of different pH was evaluated based on the release behavior of the encapsulated GFP from the core unit of the fibermats. GFP-loaded fibermats (2 mg) were placed in a 10-mL glass vial and subsequently immersed in 1.5 mL of 100 mM acetate buffer (pH 3–5), 100 mM phosphate buffer (pH 6–8), or 100 mM carbonate buffer (pH 9–10) for defined periods (0–300 min) at room temperature; the fibermats were then removed from the buffer and the UV-vis absorbance ($A$) of the remaining solution was measured (V-670, JASCO, Japan). To quantify the amount of GFP released in pH 6–10 samples, $A_{485}$, which is characteristic of GFP, was measured; for the pH 3–5 samples, the GFP released in the supernatant was quantified using the Bradford method.[21]

**Tensile-Strength Measurement of Fibermats.** For testing tensile strength, fibermats were cut into pieces of a defined size (20 mm long, 5 mm wide) and set between the sensor tips of the testing instrument (Autograph, AGS-G, Shimadzu, Japan) equipped with a 50 N load cell according to Japanese Industrial Standard (JIS L 1015). Mechanical testing was performed under the following conditions; span length 20 mm, crosshead speed 1 mm $min^{-1}$, $n = 5$.

**Contact-Angle Measurement of Fibermats.** Fibermats were stuck onto a coverslip (18 × 18 mm) and placed on the sample plate of a contact-angle measuring instrument (SImage mini7, Excimer Inc., Japan). A 5-μL droplet of water was placed on the fibermats and the shapes of the hemispherical water droplet were observed using video-image capture and the contact angles were determined; 10 samples per group were tested to determine average contact angles and standard deviations.

**Fluorescence Spectra and Emission Properties of GFP-Encapsulating Core-Shell Fibermats.** First, GFP-encapsulating core-shell fibermats were wetted with 20 mM Tris-HCl (pH 7.8) and adhered to a coverslip (20 × 20 mm, Eagle XG, Corning Inc., USA). The coverslip was then placed into the sample chamber of a FluoroMax-4 spectrofluorometer (HORIBA Scientific, Japan), and the fluorescence emission spectrum was acquired at a photoexcitation wavelength of 460 nm. To obtain fluorescence images of GFP-encapsulating fibermats, the cover slips were wetted in 100 mM phosphate buffer (pH 8) and then exposed to UV light (320 nm).

**Leakage/Release of Encapsulated Fluorescent Molecules upon Immersion in Buffer.** Loaded fibermats (2 mg) were placed in a 10-mL glass vial and immersed in 1.5 mL of 100 mM phosphate buffer (pH 8) for defined periods (0–6 h) at room temperature, after which the fibermats were removed from the buffer and the $A$ values of the remaining solutions were measured (V-670, JASCO, Japan); specifically, $A_{494}$ (characteristic of fluorescein) and $A_{554}$ (characteristic of rhodamine B) were measured to determine the degree of release of the fluorophores during the assay period.

**Enzymatic Activities of Enzyme-Encapsulating Core-Shell Fibermats.** Core-shell fibermats encapsulating α-Chy or Lac of 2.0, 4.0, or 8.0 mg were immersed in 1.5 mL of 100 mM phosphate buffer (pH 8) for the α-Chy-encapsulated fibermat or in a 50 mM Mcilvaine buffer (pH 4)[22] for the Lac-encapsulated fibermat in 10 mL glass vial for 1 h. After removal from the buffer solution, the α-Chy-encapsulating fibermats were briefly washed thrice with 100 mM phosphate buffer and placed in a 10-mL glass vial containing 3.0 mL of 100 mM phosphate buffer (pH 8); to each of these samples, 20 μL of *p*-NAc in DMSO (60 mM) was added and allowed to react for 10 min. 50 mM Mcilvaine buffer was prepared by mixing 50 mM $Na_2HPO_4$ and 50 mM citric acid. To observe the enzymatic reaction of α-Chy in the presence of TCI, TCI was added (to a final concentration of 17.5 μM) before addition of *p*-NAc. After removal of the fibermats, $A_{404}$, which is characteristic of deprotonated *p*-nitrophenol, was measured to determine the amount of *p*-nitrophenol produced based on its molar extinction coefficient (18,384 mol $cm^{-1}$ $dm^{-3}$)[23] at pH 8. In the case of Lac-encapsulating fibermats, after removal from the buffer solution, the fibermat samples were placed in 25 mM Mcllvaine buffer (pH 4) containing 5.56 mM *p*-NGlu and allowed to react for 15 min at 50 °C. After terminating the reaction by adding 4 mL of 100 mM carbonate buffer (pH 8) to the supernatant, $A_{404}$ was measured to determine the amount of *p*-nitrophenol produced (as described above for α-Chy samples). As controls, 100 mM phosphate buffer (pH 8) containing α-Chy in amounts corresponding to those in 2.0, 4.0, or 8.0 mg of α-Chy-encapsulating fibermats or 25 mM Mcllvaine buffer (pH 4) containing Lac in amounts corresponding to those in 2.0, 4.0, or 8.0 mg of Lac-encapsulating fibermats were used to determine enzymatic activities by using *p*-NAc and *p*-NGlu, respectively.

## 3. Results and Discussion

**Preparation of Core-Shell-Type Fibermats by Using a Coaxial Spinneret.** Core-shell fibermats were constructed


 

using two separately prepared precursor solutions, poly(AM/DAAM)/ADH in phosphate buffer (pH 8) and PCL in TFE, which were spun through a coaxial spinneret (Figure 1(a)) under constant voltage (details in *Experimental Section*). Several combinations of polymer species can be used to construct core-shell fibermats,[24,25] but combination of poly(AM/DAAM)/ADH and PCL was not reported yet. The chemical structures of poly(AM/DAAM), ADH, and PCL are illustrated in Figure 1(b). Poly(AM/DAAM) was synthesized through RAFT polymerization[26] of AM and DAAM by using a RAFT agent.

In the synthesized poly(AM/DAAM), the molar ratio of AM to DAAM was set to be 8:2, assigning from $^1$H NMR measurement, and the $M_n$ and PDI were determined to be 52,000 and 1.32 from GPC analysis. The $M_n$ of commercially available PCL was 80,000. The poly(AM/DAAM)/ADH solution was prepared right before electrospinning by adding ADH to poly(AM/DAAM) in phosphate buffer (pH 8). According to the progression of the crosslinking reaction between the ketone groups in poly(AM/DAAM) and the hydrazide groups in ADH, the viscosity of the solution gradually increased, but the electrospinning could be completed before the solution transformed into a stiff hydrogel (within 1.5 h). Notably, solvent volatilization (i.e., dehydration) during electrospinning can facilitate the crosslinking reaction between poly(AM/DAAM) and ADH. Thus, even in the absence of the PCL layer, the spun nanofibers could be stacked without fusion of adjacent nanofibers, and after further progression of the crosslinking reaction within each nanofiber, the obtained fibermats became water-insoluble. The feed rates of the poly(AM/DAAM)/ADH solution and PCL were fixed respectively at 0.1 and 0.4 mL/h (1:4 ratio); we also tested other spin conditions featuring distinct feed-rate ratios, but the core-shell fibermats could be successfully prepared only when this ratio was 1:3–1:4. Therefore, we selected the feed-rate ratio of 1:4 for the construction of the core-shell fibermats in this study.

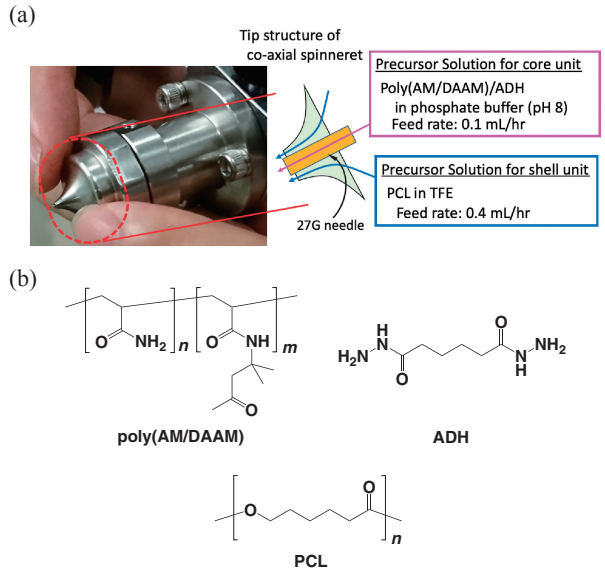


**Figure 1.** (a) Coaxial spinneret for fabrication of core-shell fibermats of poly(AM/DAAM)/ADH and PCL. (b) Chemical structures of poly(AM/DAAM), ADH, and PCL.

SEM and TEM images of the prepared core-shell fibermats are shown in Figure 2(a) and Figure 3(c), respectively. To obtain sufficient image contrast of the core unit against the shell unit in TEM images, we added a small amount (0.001 wt% against poly(AM/DAAM)) of sodium phosphotungstate to the precursor solution of the core unit before electrospinning. As a reference, we also performed TEM measurements of poly(AM/DAAM)/ADH fibermats and PCL fibermats (prepared using only PCL) (Figure 3(a), (b)). As indicated by the SEM images in Figures 2(a), we observed successful accumulation of isolated nanofibers featuring an average diameter of 473 ± 88 nm. Furthermore, a double-layered structure, consisting of the independent core and shell layers, was clearly observed at the level of the nanofibers of core-shell fibermats (Figure 3(c)). In the reference poly(AM/DAAM)/ADH fibermats and the PCL fibermats, this double-layered structure was not detected in TEM images (Figure 3(a), (b)), which strongly suggested that core-shell fibermats consisting of poly(AM/DAAM)/ADH and PCL were successfully constructed. By using the TEM images, we calculated the ratio of the average diameter (nm) of the core unit to the thickness (nm) of the shell unit to be 3.69 ± 0.81. The fiber diameters in TEM samples appeared smaller than those in SEM samples, but this can be explained according to the method used to prepare TEM samples; in order to get the TEM sample of single nanofibers, we collected nanofibers at the interspace between the spinneret needle and plate-collector to shorten the collecting time of nanofibers. Due to difference of preparation procedure the average diameter of the observed nanofibers was different, but the estimated ratio of the core diameter and the shell thickness should be similar to those of core-shell fibermats collected on a plate-collector.

We next used ATR-IR measurements to further characterize the core-shell fibermats (Figure 4). In our previous study on the

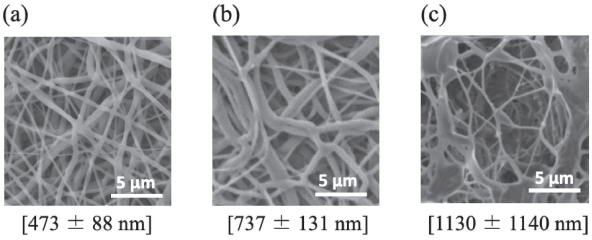


**Figure 2.** SEM images of the core-shell fibermats of poly(AM/DAAM)/ADH and PCL (a) before and (b) after immersion in 50 mM phosphate buffer (pH 8) for 1 h, and of (c) poly(AM/DAAM)/ADH fibermats after immersion in the buffer. Acceleration voltage, 10 kV.

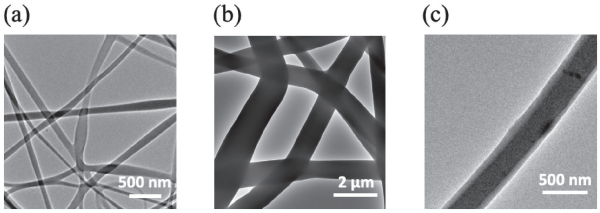


**Figure 3.** TEM images of (a) poly(AM/DAAM)/ADH fibermat, (b) PCL fibermat, and (c) the core-shell fibermat of poly(AM/DAAM)/ADH and PCL. Acceleration voltage, 200 kV.

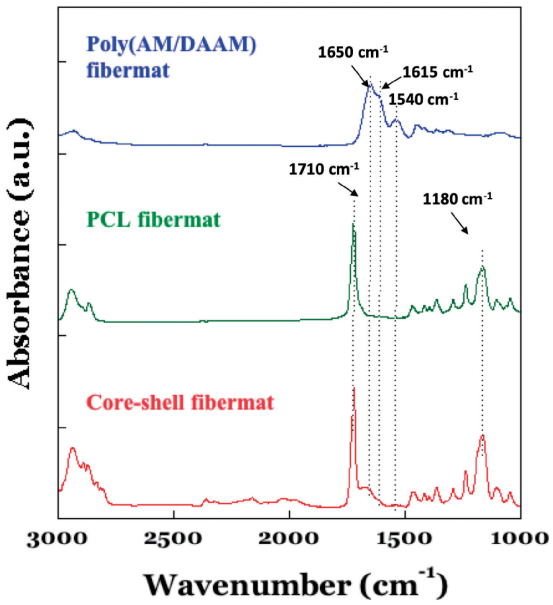


**Figure 4.** ATR-IR spectra of poly(AM/DAAM)/ADH fibermats (blue line), PCL fibermats (green line), and core-shell fibermats (red line).

poly(AM/DAAM)/ADH fibermat, according to the formation of hydrazone bonds between the ketone groups in poly(AM/DAAM) and the hydrazide groups in ADH, IR bands emerged at 1540 and 1615 $cm^{-1}$ in addition to the IR band for the amide bond in AM and DAAM at 1650 $cm^{-1}$.[15] Since similar IR bands were also observed for the core-shell fibermat in Figure 4, crosslinking reaction between the ketone groups in poly(AM/DAAM) and the hydrazide groups in ADH also occurred. With the core-shell fibermats, besides the aforementioned IR bands, we detected the coexistence of other IR bands, at 1710 and 1180 $cm^{-1}$, corresponding to the ester bonds in PCL.[27] The coexistence of these IR bands also suggested successful construction of the target core-shell fibermats of poly(AM/DAAM)/ADH and PCL.

Measurement of the contact angle of water droplets is another effective method to verify PCL wrapping of the core unit of poly(AM/DAAM)/ADH in core-shell fibermats. If the poly(AM/DAAM)/ADH core is successfully wrapped with the PCL layer without any defect, the obtained core-shell nanofibers would be expected to show altered hydrophobicity, originating from the hydrophobic nature of PCL. Water droplets spotted on top of fibermats and the calculated average contact angles are shown in Figure 5 and Table 1, respectively. Reflecting the hydrophilic nature of poly(AM/DAAM)/ADH, the contact angle of the poly(AM/DAAM)/ADH fibermat was first measured to be 17° ± 6.3°, and according to adsorption of water, this value decreased further. By contrast, the contact angle of the core-shell fibermat was observed to be 119° ± 3.5° with no change, which is comparable to that of PCL fibermats (125° ± 1.6°). These data also suggested successful preparation of the core-shell fibermats of poly(AM/DAAM)/ADH and PCL.

Because of the inherent properties of PCL, wrapping of the nanofibers of poly(AM/DAAM)/ADH with PCL (i.e., preparation of the core-shell fibermats) was expected to substantially

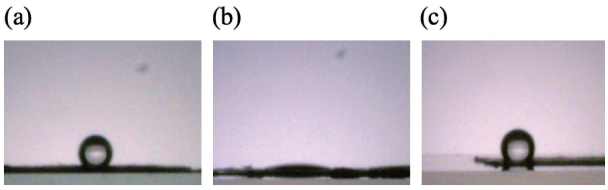


**Figure 5.** Images showing water droplets placed onto (a) core-shell fibermat, (b) poly(AM/DAAM)/ADH fibermat, and (c) PCL fibermat.

**Table 1.** Contact Angles of Distinct Fibermats for Water Droplets

| Fibermat sample | Contact angle (°) |
|---|---|
| PCL fibermat | 125 ± 1.6 |
| Poly(AM/DAAM)/ADH fibermat | 17 ± 6.3 |
| Core-shell fibermat | 119 ± 3.5 |

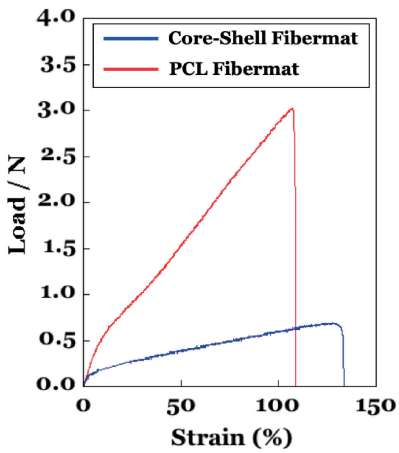


**Figure 6.** Tensile-strength measurement of PCL fibermat and core-shell fibermat of poly(AM/DAAM)/ADH and PCL.

enhance the mechanical strength of the fibermats against tensile forces. Therefore, we next examined maximum load value (N) under the application of tensile strain (%) to dumbbell-shaped samples of core-shell fibermats by using a tensile test instrument. The obtained data are summarized in Figure 6 and Table 2. The poly(AM/DAAM)/ADH fibermat was extremely soft and fragile, and thus the maximum load value could not be determined. Conversely, for the core-shell fibermat of poly(AM/DAAM)/ADH and PCL, the maximum load value was able to obtain and estimated to be 0.67 ± 0.04 N. As expected, the tensile strength of the core-shell fibermat was adequately raised by PCL wrapping.

To ascertain whether the use of the PCL wrapping would enhance the long-term stability of stacked nanofibrous structures in an aqueous buffer, we performed SEM analyses on poly(AM/DAAM)/ADH fibermats and the core-shell fibermats of poly(AM/DAAM)/ADH and PCL before and after immersion in a buffer for 1 h (Figure 2(b), (c)). In the case of poly(AM/DAAM)/ADH fibermats, although a stacked structure of nanofibers was retained, partial fusion between adjacent nanofibers was observed (Figure 2(c)); by contrast, no nanofiber


 

**Table 2.** Results of Tensile Tests of Fibermats

| Fibermat sample | Maximum load/N | Elongation to failure (%) |
|---|---|---|
| PCL fibermat | 3.21 ± 0.14 | 112 ± 8.2 |
| Poly(AM/DAAM)/ADH fibermat | Not obtained (extremely fragile) | |
| Core-shell fibermat | 0.67 ± 0.04 | 133 ± 5.3 |

fusion was detected for the core-shell fibermat (Figure 2(b)). Intriguingly, after immersion in the buffer, increase (by ~30%) in the average diameter of the core-shell nanofibers was observed, which could be caused by the swelling of the core unit of poly(AM/DAAM)/ADH in the immersion buffer.

**Characterization of GFP-Encapsulating Core-Shell Fibermats.** By PCL wrapping (i.e. modifying the original poly(AM/DAAM) fibermat to the core-shell fibermat with PCL), we successfully enhanced the tensile strength of the poly(AM/DAAM)/ADH nanofibers (i.e., of the core unit of the core-shell fibermats) and the long-term stability of the stacked nanofibrous structure after immersion in a buffer. Therefore, we next move to protein encapsulation experiments. Because stable retention of enzyme molecules in the core unit without leakage is indispensable for evaluation of their biological activities, we first assessed the release behavior of encapsulated proteins after immersion in buffers of distinct pH. As a probe protein, we used GFP (Figure 7),[28] which allows easy observation of protein leakage by monitoring GFP fluorescence. Moreover, GFP encapsulation in polymeric materials has been widely attempted and the relationship between GFP fluorescence properties and the impact of encapsulation on protein structure and biological activities discussed.[29] From the fluorescence emission properties, we could estimate the effects of encapsulation in the core unit of core-shell fibermat on protein structure and functions of encapsulating enzyme molecules.

GFP was encapsulated in the core unit of core-shell fibermats through simple addition of GFP to the precursor phosphate buffer (pH 8) of 20 wt% poly(AM/DAAM)/ADH (GFP content was fixed at 5 wt% relative to that of poly(AM/DAAM)). Coaxial electrospinning was performed using the same method as that used to construct the core-shell fibermat without protein. A representative SEM image, TEM image, and the ATR-IR spectrum of the obtained GFP-encapsulating core-shell fibermat are illustrated in Figure 7(a), Figure 7(b), and Figure 8, respectively. Although the average diameter of the obtained core-shell fibermat was slightly increased and the ratio of the average diameter (nm) of the core unit to the thickness (nm) of the shell unit becoming larger than that without protein (7.24 ± 1.50), a stacked nanofibrous structure (Figure 7(a)) and the characteristic IR bands at 1710, 1650, 1615, 1540, and 1180 $cm^{-1}$ (Figure 8) were observed. These results indicate that GFP addition to the precursor solution of the core unit did not affect the construction of the core-shell fibermats of poly(AM/DAAM)/ADH and PCL. Furthermore, examination of the emission behavior and fluorescence spectrum of the encapsulated GFP (Figure 7(b)) revealed that the GFP $\lambda_{max}$ (510 nm) in the core-shell fibermat was identical to that in a buffer, which suggests that the original fluorescence property of GFP was

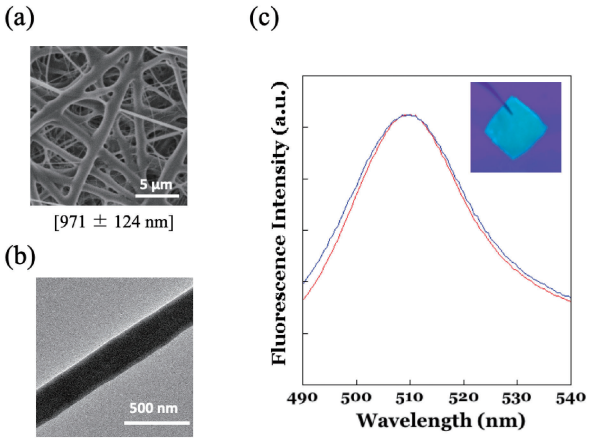


**Figure 7.** (a) SEM image of GFP-encapsulating core-shell fibermat. Osmium oxide vapor was deposited onto the fibermat sample. Acceleration voltage, 5 kV. (b) TEM image of GFP-encapsulating core-shell fibermat. The core unit was stained with phosphotungstate-Na, Acceleration voltage, 200 kV. (c) Fluorescence emission of encapsulated GFP (red line) in core-shell fibermats. The reference fluorescence spectrum of GFP in a phosphate buffer (pH 7) was illustrated as blue line in the same figure.

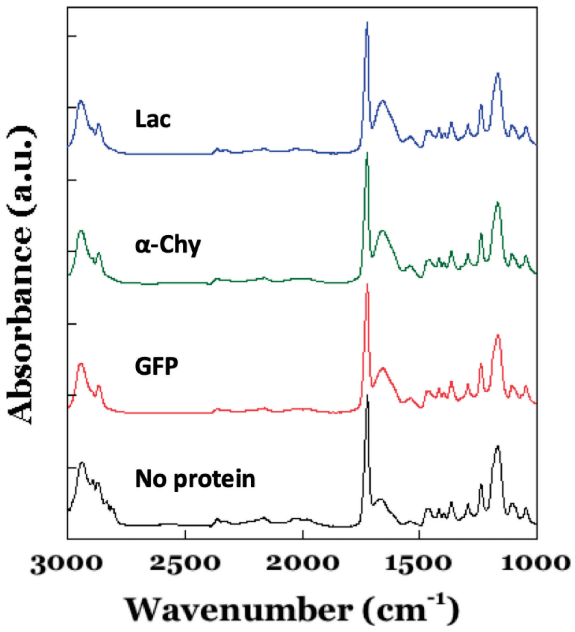


**Figure 8.** ATR-IR spectra of core-shell fibermats incorporating no protein (black line) or encapsulating GFP (red line), α-Chy (green line), or Lac (blue line).

maintained even after encapsulation. Furthermore, the homogeneous GFP emission from the fibermats implied homogeneous distribution of GFP molecules in the core unit of the core-shell fibermats. These data implied that other proteins such as enzymes could also be encapsulated in the core unit of core-shell fibermats without protein denaturation.

We next analyzed the leakage behavior of the encapsulated GFP into immersion buffers of different pH. Based on our previous analysis of the poly(AM/DAAM)/ADH fibermat,[13] poly(AM/DAAM)/ADH in the core unit was expected to

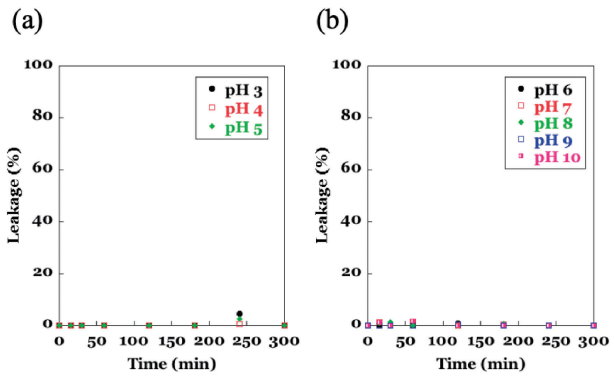


**Figure 9.** Release behavior of encapsulated GFP from GFP-encapsulating core-shell fibermats upon immersion in buffers of (a) pH 3–5 and (b) pH 6–10.

dissolve in an acidic buffer (pH <5) according to the hydrolysis of hydrazone bonds. Conversely, GFP was expected to be stably retained in neutral or slightly basic buffers because the network structure of poly(AM/DAAM)/ADH layer is not damaged under these conditions. The obtained profile of GFP leakage from the core-shell fibermat into immersion buffers is summarized in Figure 9. As expected, under neutral and slightly basic conditions, no release of GFP was observed. While, even under acidic conditions (pH < 5), GFP release was not observed. Because the hydrophobic PCL layer was insoluble in all tested buffers of different pH, GFP likely remained entrapped in the hollow tubular PCL shell layers.

**Characterization of Enzyme-Encapsulating Core-Shell Fibermats.** Lastly, we constructed enzyme-encapsulating core-shell fibermats and characterized their biological activities. For evaluating the biological activities of the enzymes encapsulated in core-shell fibermats, it was necessary to first assess the permeability of substrate molecules for enzymes into the fibermats, because molecular permeation could potentially be impeded by the PCL wrapping. Therefore, we constructed core-shell fibermats encapsulating the low-MW molecule fluorescein (MW = 332) or rhodamine B (MW = 479) as dummy fluorescent molecules in the core unit of the fibermats and assessed their release behaviors. If robust release of these encapsulated molecules from the core unit to immersion buffers was observed, adequate permeation of the substrate molecules having similar MW from the immersion buffers to the inside of the core unit was expected. The observed release behaviors into an immersion buffer are summarized in Figure 10. As compared with poly(AM/DAAM) fibermats,[15] which lacked the PCL wrapping, the release rate and release amount were slightly decreased. Nevertheless, with fluorescein, the release was found to be sufficient (>60%) and to rapidly reach equilibrium (within 30 min) (Figure 10), which suggested that if low-MW substrates are used, enzymatic activities of enzyme-encapsulating core-shell fibermats can be evaluated.

Considering the aforementioned results, we next selected two representative pairs of enzyme and substrate; α-Chy[30] and *p*-NAc (MW = 181), and Lac[31] and *p*-NGlu (MW = 301) (Figure 11) and constructed the corresponding enzyme-encapsulating core-shell fibermats. In both cases, measurement of $A_{404}$ (characteristic of *p*-nitrophenolate) enabled spectrophotometric monitoring of the amounts of products generated by the enzymes,[23] which allowed evaluation of apparent enzymatic activities.

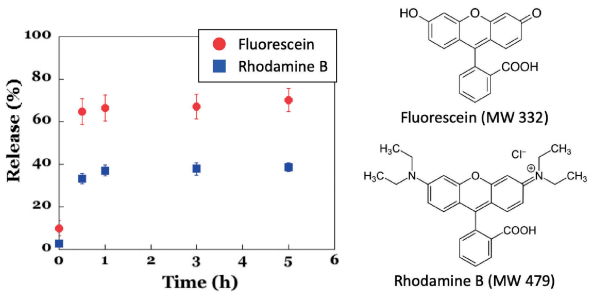


**Figure 10.** Release behaviors of fluorescein and rhodamine B from core-shell fibermats encapsulating either molecule in the core unit.

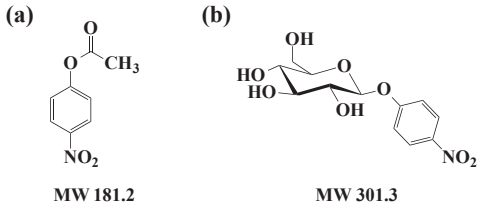


**Figure 11.** Chemical structure of (a) p-nitrophenyl acetate and (b) p-nitrophenyl-β-D-glucoside.

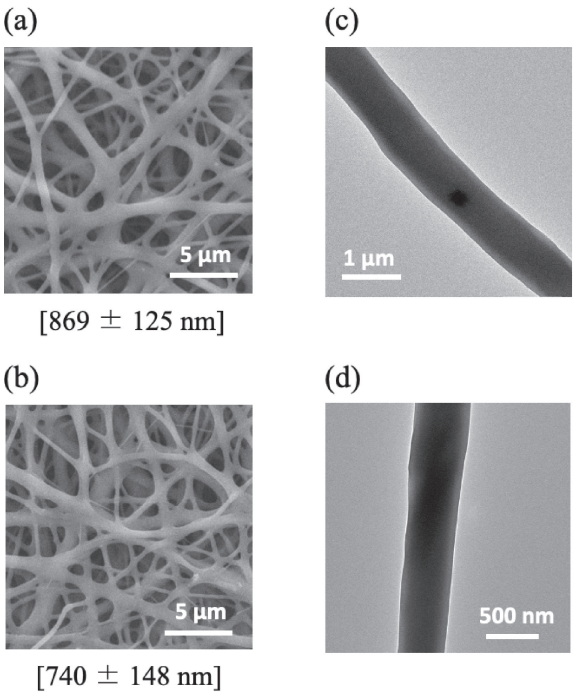


**Figure 12.** SEM and TEM images of the core-shell fibermats encapsulating α-Chy ((a), (c)) and Lac ((b), (d)). For TEM measurements, the core unit was stained with phosphotungstate-Na, Acceleration voltage, 200 kV.

Core-shell fibermats encapsulating α-Chy or Lac were constructed similarly as GFP-encapsulating fibermats. The ATR-IR spectra, SEM images, and TEM images of these fibermats are displayed in Figure 8 and Figure 12, respectively. Although the ratio of the average diameter (nm) of the core unit to the


 

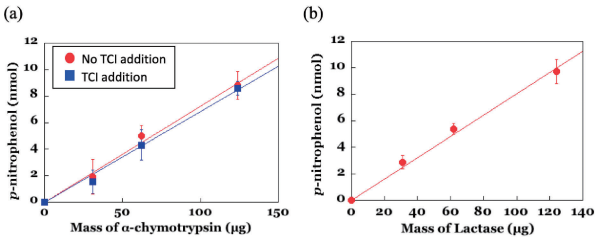


**Figure 13.** Plots showing *p*-nitrophenol amounts (nmol) produced in 10 min against amounts of (a) α-Chy or (b) Lac in the core unit of core-shell fibermats.

**Table 3.** Apparent enzymatic activities of core-shell fibermats encapsulating α-Chy in the presence/absence of TCI or encapsulating Lac: Comparison with enzymes dissolved in assay buffer

| | Apparent enzymatic activity (nmol min$^{-1}$ mg$^{-1}$) | | |
|---|---|---|---|
| | α-Chymotrypsin | | Lactase |
| | No TCI | Presence of TCI | |
| Buffer | 8.95 ± 0.91 | 0.28 ± 0.03 (97% deactivated)[b] | 7.73 ± 0.20 |
| Poly(AM/DAAM) /ADH fibermat | 7.83 ± 0.25 (87%)[a] | 5.34 ± 0.29 (32% deactivated)[b] | — |
| Core-shell fibermat | 7.24 ± 1.08 (81%)[a] | 6.84 ± 0.81 (6% deactivated)[b] | 5.38 ± 0.52 (70%)[a] |

[a]These values were calculated in comparison with values measured in buffer. [b]These values were calculated in comparison with values, measured in the absence of TCI.

thickness (nm) of the shell unit became larger than that without protein (6.14 ± 0.80 for α-Chy, 5.30 ± 0.48 for Lac), the obtained data indicated that encapsulation of neither enzyme markedly affected the construction of core-shell fibermats of poly(AM/DAAM)/ADH and PCL. On the other hand, that the ratio of core diameter to shell thickness is over 5 means that, even if the protein-loaded nanofibers had 1 μM of diameter, still shell thickness is less than 150 nm. In terms of enzyme reactivity, this characteristic was expected to have advantages.

Enzymatic activities of the encapsulated enzymes were evaluated from the product amounts in a 10-min reaction by using different weights of enzyme-encapsulating core-shell fibermats (i.e., by using different weights of enzyme samples encapsulated in the core-shell fibermats). In linear-fitting analyses of the data collected from these samples (Figure 13), the enzymatic activities were estimated as the slopes of the obtained plots, and nmol min$^{-1}$ mg$^{-1}$ was used as the activity unit (1 U = 1 mg of enzyme sample that produces 1 nmol of enzymatic product within 1 min). In control experiments, we also evaluated enzymatic activity by using an identical amount of α-Chy or Lac dissolved directly in the assay buffer. The estimated enzymatic activities from the observed data are summarized in Table 3. In our previous study on the poly(AM/DAAM)/ADH fibermat, we found that α-Chy-encapsulating poly(AM/DAAM)/ADH fibermats exhibited >85% apparent enzymatic activity relative to that of the same amount of enzyme dissolved in buffer.[15] Because of the porous network structure of poly(AM/DAAM)/ADH and the high surface area of the stacked nanofibrous structure of α-Chy-encapsulating poly(AM/DAAM)/ADH fibermats, apparent enzymatic activity successfully reached >85%. Although hinderance of substrate permeation due to the PCL wrapping was a major concern, we unexpectedly found that the α-Chy-encapsulating core-shell fibermats exhibited nearly 80% apparent enzymatic activity relative to that of the same amount of enzyme dissolved in buffer. In the case of Lac-encapsulating core-shell fibermats, the activity reached 70% relative to that in buffer. As our discussion of GFP-encapsulating core-shell fibermats in the preceding section, α-Chy and Lac in the core unit of the core-shell fibermats might retain their original structure and function in the fibermats. Therefore, the small reduction observed here in enzymatic activities (i.e., the reduction in apparent enzymatic activities) is likely due to a decrease in the molecular permeability of the substrate molecules.

One of the advantages of encapsulating enzymes in the nanofibers of fibermats is that the enzymes are protected from undesirable interactions with contaminating molecules in biological samples, such as inhibitory peptides and proteases. Because of the filtering effect originating from the PCL wrapping in the shell unit and the network structure of poly(AM/DAAM)/ADH in the core unit, we expected the access of middle- or high-MW molecules (>1 kDa) to the encapsulated enzyme in the core unit to be suppressed. As a pilot experiment, we evaluated the effect of an inhibitory peptide, TCI,[20] on the enzymatic activity of α-Chy either encapsulated in the core-shell fibermat or dissolved in a buffer. TCI is a linear 7.9-kDa peptide that can form a 1:1 complex with α-Chy in solution. After this 1:1 binding, α-Chy enzymatic activity was strongly inhibited (97% of the original activity was suppressed; Table 3). In our previous study on the poly(AM/DAAM)/ADH fibermat, α-Chy encapsulation in the fibermat protected the original α-Chy activity by 68%; inclusion of α-Chy in the network structure of poly(AM/DAAM)/ADH hindered the TCI approach, but a certain level of TCI binding and the subsequent inhibition still remained.[15] By comparison, in the case of the core-shell fibermats, only 6% of the original enzymatic activity of α-Chy was inhibited. The double-layered fibrous structure of the core-shell fibermats, consisting of the PCL shell and the network structure of poly(AM/DAAM)/ADH, provided clearly superior protection of α-Chy against TCI binding. This type of protection of the biological functions of proteins against the effects of middle- or high-MW molecules (>1 kDa) is likely to be a general behavior encountered when using the core-shell fibermats. Additional optimization of fibermat nanostructure and selection of polymer species can potentially further enhance the performance of these fibermats relative to that demonstrated for protein-encapsulating single-layered fibermats.

## 4. Conclusion

In this study, we characterized enzyme-encapsulating core-shell fibermats in which enzyme molecules (of α-Chy or Lac) were included in the core unit of poly(AM/DAAM)/ADH and a PCL layer was wrapped around this core unit. Distinct from the enzyme-encapsulating poly(AM/DAAM)/ADH fibermat composed of only the poly(AM/DAAM)/ADH layer including enzyme molecules, the core-shell fibermat exhibited sufficient mechanical strength and stability of the stacked nanofibrous

structure in a neutral-pH buffer, with both of these characteristics originating from the hydrophobic shell unit of PCL. Furthermore, the thin PCL wrapping (<150 nm thick) of the poly(AM/DAAM)/ADH layer did not markedly impede the permeation of low-MW substrates. Thus, the enzyme-encapsulating core-shell fibermats functioned effectively in allowing entry of low-MW substrates while concurrently suppressing the adverse impact of middle- or high-MW (>1 kDa) contaminating molecules such as inhibitor peptides and proteases; the apparent enzymatic activities of α-Chy-encapsulating and Lac-encapsulating fibermats reached 81% and 70%, respectively, relative to activities of the same amounts of the enzymes dissolved in buffer. These results imply that core-shell fibermats of poly(AM/DAAM)/ADH (core unit) and PCL or other hydrophobic polymers (shell unit) could emerge as a novel class of enzyme-immobilizing platforms. Our group is now comprehensively evaluating enzyme-encapsulating core-shell fibermats generated using distinct combinations of polymers.

This work was supported by JSPS KAKENHI (Grant Number 17K05932), and the TOYOAKI SCHLORSHIP FOUNDATION, and the NIMS Molecule & Material Synthesis Platform in the "Nanotechnology Platform Project" operated by the Ministry of Education, Culture, Sports, Science and Technology (MEXT).

## References

1 R. Jayakumar, S. Nair, ed., *Biomedical Applications of Polymeric Nanofibers*; Springer: Berlin, Heidelberg, Germany, 2012.
2 L. Tian, M. P. Prabhakaran, X. Ding, D. Kai, S. Ramakrishna, *J. Mater. Sci.: Mater. Med.* **2013**, *24*, 2577.
3 M. G. Lancina, III, R. K. Shankar, H. Yang, *J. Biomed. Mater. Res., Part A* **2017**, *105*, 1252.
4 Y. Dai, J. Niu, J. Liu, L. Yin, J. Xu, *Bioresour. Technol.* **2010**, *101*, 8942.
5 H. Qi, P. Hu, J. Xu, A. Wang, *Biomacromolecules* **2006**, *7*, 2327.
6 M. Monfared, S. Taghizadeh, A. Zare-Hoseinabadi, S. M. Mousavi, S. A. Hashemi, S. Ranjbar, A. M. Amani, *Drug Metab. Rev.* **2019**, *51*, 589.
7 S. Zupančič, *Acta Pharm.* **2019**, *69*, 131.
8 Y. Yang, X. Li, W. Cui, S. Zhou, R. Tan, C. Wang, *J. Biomed. Mater. Res., Part A* **2008**, *86A*, 374.
9 G. Ren, X. Xu, Q. Liu, J. Cheng, X. Yuan, Y. Wan, *React. Funct. Polym.* **2006**, *66*, 1559.
10 H. Bang, K. Watanabe, R. Nakashima, W. Kai, K.-H. Song, J. S. Lee, M. Gopiraman, I.-K. Kim, *RSC Adv.* **2014**, *4*, 59571.
11 P. Gupta, S. Trenor, T. E. Long, G. L. Wilkes, *Macromolecules* **2004**, *37*, 9211.
12 M. Kurecic, T. Mohan, N. Virant, U. Maver, J. Stergar, L. Gradisnik, K. S. Kleinschek, S. Hribernik, *RSC Adv.* **2019**, *9*, 21288.
13 S. Koeda, K. Ichiki, N. Iwanaga, K. Mizuno, M. Shibata, A. Obata, T. Kasuga, T. Mizuno, *Langmuir* **2016**, *32*, 221.
14 K. Mizuno, S. Koeda, A. Obata, J. Sumaoka, T. Kasuga, J. R. Jones, T. Mizuno, *Langmuir* **2017**, *33*, 4028.
15 Y. Ido, A. L. B. Maçon, M. Iguchi, Y. Ozeki, S. Koeda, A. Obata, T. Kasuga, T. Mizuno, *Polymer* **2017**, *132*, 342.
16 Z. Sun, Z. E. Alexander, A. L. Yarin, J. H. Wendroff, A. Greiner, *Adv. Mater.* **2003**, *15*, 1929.
17 N. Han, P. A. Bradley, J. Johnson, K. S. Parikh, A. Hissong, M. A. Calhoun, J. J. Lannutti, J. O. Winter, *J. Biomater. Sci., Polym. Ed.* **2013**, *24*, 2018.
18 S. Srouji, D. Ben-David, R. Lotan, E. Livne, R. Avrahami, E. Zussman, *Tissue Eng. Part A* **2011**, *17*, 269.
19 C. L. McCormick, A. B. Lowe, *Acc. Chem. Res.* **2004**, *37*, 312.
20 Y. Birk, *Int. J. Pept. Protein Res.* **1985**, *2*, 113.
21 T. Zor, Z. Selinger, *Anal. Biochem.* **1996**, *236*, 302.
22 T. C. McIlvaine, *J. Biol. Chem.* **1921**, *49*, 183.
23 A. E. Beg, *J. Chem. Soc. Pak.* **1984**, *6*, 55.
24 Y. Zhang, Z.-M. Huang, X. Xu, C. T. Lim, S. Ramakrishna, *Chem. Mater.* **2004**, *16*, 3406.
25 N. Han, J. K. Johnson, P. A. Bradley, K. S. Parikh, J. J. Lannutti, J. O. Winter, *J. Funct. Biomater.* **2012**, *3*, 497.
26 P. Wen, Y. Wen, X. Huang, M. H. Zong, H. Wu, *J. Agric. Food Chem.* **2017**, *65*, 4786.
27 T. Elzein, M. Nasser-Eddine, C. Delaite, S. Bistac, P. Dumas, *J. Colloid Interface Sci.* **2004**, *273*, 381.
28 J. D. Pédelacq, S. Cabantous, T. Tran, T. C. Terwilliger, G. S. Waldo, *Nat. Biotechnol.* **2006**, *24*, 79.
29 J. N. Brantley, C. B. Bailey, J. R. Cannon, K. A. Clark, D. A. Vanden Bout, J. S. Brodbelt, A. T. Keatinge-Clay, C. W. Bielawski, *Angew. Chem., Int. Ed.* **2014**, *53*, 5088.
30 F. J. Kezdy, M. L. Bender, *Biochemistry* **1962**, *1*, 1097.
31 M. M. Maksimainena, A. Lampio, M. Mertanen, O. Turunen, J. Rouvinen, *Int. J. Biol. Macromol.* **2013**, *60*, 109.


 